Available online at www.sciencedirect.com
SCIENCE DIRECT
Journal of Catalysis 241 (2006) 304–311
JOURNAL OF CATALYSIS
www.elsevier.com/locate/jcat

Xylene isomerization with surface-modified HZSM-5 zeolite catalysts: An in situ IR study

Shourong Zheng [a], Andreas Jentys [b,*], Johannes A. Lercher [b]

[a] *State Key Laboratory of Pollution Control and Resource Reuse, School of Environment, Nanjing University, Nanjing, 210093, PR China*
[b] *Technische Universität München, Lehrstuhl II für Technische Chemie, Lichtenbergstr. 4, D-85747 Garching, Germany*

Received 23 December 2005; revised 20 April 2006; accepted 21 April 2006

Available online 9 June 2006

Abstract

Xylene isomerization over parent and *tetra*-ethoxysilane-modified HZSM-5 was studied using time-resolved in situ IR spectroscopy to monitor the concentrations of reactants and products inside the pores. Surface silylation formed patches sealing pore mouths, enhancing the differences in diffusivity between *p*-xylene and *o*- or *m*-xylene via increased tortuosity of the transport pathway. The reaction rate of *m*-xylene isomerization was controlled by reactant diffusion; the selectivity, by restrictions in the transition state. For *p*- and *o*-xylene isomerization over the silylated zeolite, the greater local concentration of the reaction intermediate *m*-xylene compared with that of the reactant molecules in the pores indicated that the bulkiest isomer (i.e., *m*-xylene) was selectively retained in the pores. Its higher effective residence time in the pores allowed conversion to *p*- and *o*-xylene. Because *p*- and *o*-xylene were formed from *m*-xylene in a ratio of approximately 2, this led to enhanced *p*-xylene selectivity. Xylene isomerization catalyzed by Brønsted acid sites in the pore mouth of the zeolite was largely suppressed after silylation.

Keywords: Zeolites; Shape selectivity; Xylene isomerization; In situ IR spectroscopy; Surface reactions; Reaction mechanism

1. Introduction

HZSM-5 zeolite is widely used as a shape-selective catalyst in several industrial processes, including alkylation, isomerization, and disproportionation [1–5]. However, HZSM-5 and especially materials with small crystals show moderate to low selectivity to *p*-xylene [6,7], which usually can be enhanced by postsynthetic modification. Among these methods, chemical vapor deposition (CVD) [8–10] and chemical liquid deposition (CLD) [11,12] of silica on the external surface of HZSM-5 have proven to be the most effective approaches for preparing stable and highly selective catalysts. In general, silylation using *tetra*-ethoxysilane (TEOS) or *tetra*-methoxysilane (TMOS) leads to a narrowing and/or blocking of the pore openings and simultaneously to the passivation of acid sites in the pore mouth region of HZSM-5. High *p*-selectivity of HZSM-5 in xylene isomerization is attributed to the greater diffusivity of *p*-xylene compared with that of *o*- or *m*-xylene (product shape selectivity). For smaller crystals, however, reactants and primary products isomerize in the pores and have sufficiently short diffusion pathways for leaving the zeolite crystallites, or isomerize at sites directly at the pore mouth region, leading to a mixture of xylenes close to the thermodynamic equilibrium. But through blocking or narrowing of pores, the diffusion of *o*- and *m*-isomers out of the pores is retarded and/or isomerization catalyzed by acid sites at the pore entrance is suppressed [12–16], thus enhancing the selectivity to *p*-substituted products.

We have already successfully applied time-resolved in situ IR spectroscopy to follow the influence of xylene diffusion on the activity and selectivity of HZSM-5 zeolites for xylene isomerization [17–19]. The studies showed that *m*-xylene isomerization is controlled primarily by restricted transition state selectivity, whereas for *o*- and *p*-xylene isomerization, the lower diffusivity of *m*-xylene leads to retention of the primary product *m*-xylene, resulting in higher selectivity via product diffusion control. The present contribution extends these studies to include the effects of the postsynthetic modification by silylation

* Corresponding author.
E-mail address: andreas.jentys@ch.tum.de (A. Jentys).

0021-9517/$ – see front matter
doi:10.1016/j.jcat.2006.04.026

with TEOS and the role of reactions in the pore mouth region. Here the current models for describing the transport and sorption of aromatic molecules in HZSM-5 [30,37,38] are combined with in situ IR spectroscopy to develop a detailed mechanistic description of the isomerization reaction inside the pores and at the pore entrances.

2. Experimental

2.1. Materials

HZSM-5 zeolite with a Si/Al ratio of 45 and an average particle size of 0.5 μm, determined by scanning electron microscopy, was used as the parent zeolite.

2.2. Silylation

Typically, 2 g of zeolite was suspended in 50 mL of hexane, and the mixture was heated under stirring until reflux. Then 0.3 mL of TEOS, corresponding to a loading of 4 wt% SiO_2, was introduced into the mixture, and the silylation was carried out for 1 h under reflux and stirring. Subsequently, hexane was removed by evacuation. The sample was dried at 393 K for 2 h and calcined at 773 K for 4 h in dry air. Three-cycle silylation of the zeolite was carried out by repeating the foregoing procedure three times. The parent and the three-cycle silylated zeolites are termed HZSM-5 and HZSM-5M, respectively. The properties of the parent and modified zeolite were described previously [13]; the acid site densities of the parent and modified zeolites determined by NH_3 temperature-programmed desorption were 0.30 and 0.23 mmol/g, respectively.

2.3. Measurements of diffusivity

The diffusivities of *p*-, *o*-, and *m*-xylene in the parent and silylated zeolites were determined using infrared (IR) spectroscopy in a flow IR system as described previously [17]. The IR spectra were collected on a Bruker IFS 88 Fourier transform IR spectrometer at a resolution of 4 cm^{-1}.

For a typical measurement, the zeolite was pressed into a self-supporting wafer, which was then placed inside a gold sample holder surrounded by a heating wire. The sample holder was mounted in the center of an in situ cell connected to a flow system. The sample was activated by heating to 823 K in helium flow at a rate of 10 K/min and holding this temperature for 1 h. After the sample temperature was stabilized at 373 K, xylene with a partial pressure of 1 mbar was injected into the He flow using a syringe pump, and the IR spectra were collected at 15-s intervals. The diffusion coefficients were estimated using the following formula [20,21]:

$$Q_t/Q_\infty = 6/r_0(Dt/\pi)^{1/2},$$

where Q_t is the amount adsorbed at time t (in s), Q_∞ is the amount adsorbed at equilibrium coverage, r_0 is the radius of the zeolite crystal, and D is the diffusion coefficient.

The normalized areas of the IR bands of *p*-xylene at 1516 cm^{-1}, *o*-xylene at 1497 and 1468 cm^{-1}, and *m*-xylene at 1610 cm^{-1} were used to quantify the relative concentrations of adsorbate in the zeolites. The IR spectra collected indicated the absence of isomerization reactions at 373 K. The overtone and combination vibrations of HZSM-5 zeolite at 1990 and 1870 cm^{-1} were used to normalize the intensity of the IR bands.

2.4. In situ IR spectroscopy of xylene isomerization

Isomerization of *o*-, *m*-, or *p*-xylene was carried out in an in situ flow cell having the characteristics of a continuously operated stirred-tank reactor [17,18]. Typically, a self-supporting wafer of the zeolite was activated at 823 K for 1 h. At the reaction temperature, xylene with a partial pressure of 20 mbar was introduced into the He stream. The surface species formed on the zeolites were followed by IR spectra measured at 15-s intervals during xylene isomerization. The product composition of xylene isomerization in the reactor was simultaneously measured by on-line gas chromatography using a 16-loop sampling valve to decouple analysis and sampling time intervals. To determine the concentration of the species in the zeolite pores, the IR spectra were fitted with a linear combination using the IR spectra of the three xylene isomers adsorbed on silica. The molar extinction coefficients of the adsorbed reactants and products were determined as described previously [17].

3. Results

3.1. Diffusion of xylenes

The time-solved IR spectra of *o*-xylene adsorbed in the parent zeolite are shown in Fig. 1. With increasing exposure, the intensity of the IR bands at 3745 and 3606 cm^{-1} decreased, indicating the interaction of *o*-xylene with the silanol and bridging hydroxyl groups via hydrogen bonding. Simultaneously, IR bands characteristic for *o*-xylene at 1497, 1468, and around 3000 cm^{-1}, as well as a broad band at 3168 cm^{-1} characteristic for perturbed bridging hydroxyl groups, were observed. The changes in the intensity of the IR bands at 1497 and 1468 cm^{-1} during *o*-xylene adsorption over the parent and silylated zeolites as a function of adsorption time are compiled in Fig. 2. The adsorption of *o*-xylene over the parent zeolite reached the equilibrium after about 1800 s, whereas even after 3000 s, only 50% of the sorption capacity of the silylated zeolite was reached, indicating a markedly slower diffusivity of *o*-xylene into the silylated zeolite compared with that over the parent zeolite.

The diffusion coefficients of the xylene isomers at 373 K and 1 mbar (calculated from the data shown in Fig. 2) on the parent and silylated zeolites are compiled in Table 1. In the parent zeolite, the diffusion coefficient of *p*-xylene was approximately one to two orders of magnitude higher than those of *o*- and *m*-xylene. Because the kinetic diameters of *p*-, *o*-, and *m*-xylene and the pore diameter of HZSM-5 zeolites are in the same order, the diffusion of xylenes into HZSM-5 can be considered configurational diffusion [22,23]. Therefore, the greater diffusivity of *p*-xylene is related to its smaller kinetic diameter (0.58 nm) compared with that of *o*-xylene (0.68 nm) and

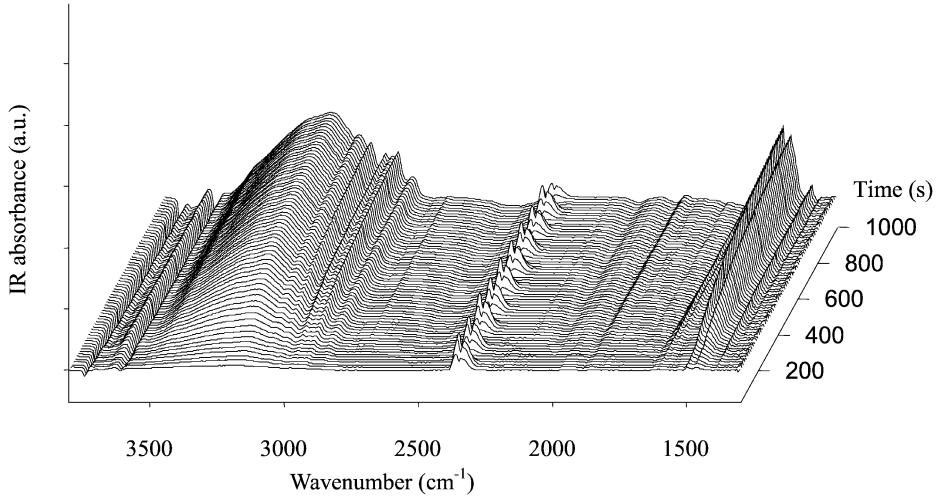

Fig. 1. Time resolved IR spectra of *o*-xylene adsorption on HZSM-5 at 373 K and 1 mbar.

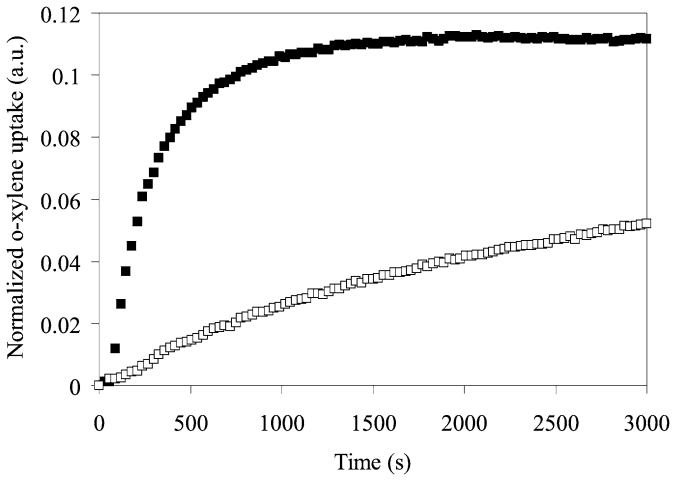

Fig. 2. Uptakes of *o*-xylene on HZSM-5 (■) and HZSM-5M (□) at 373 K and 1 mbar.

Table 1
Diffusion coefficients of xylenes at 373 K and 1 mbar over the parent and silylated zeolite and from literature [17]

Sample	Crystal size (μm)	*p*-Xylene ($\times 10^{-17}$ m^2/s)	*o*-Xylene ($\times 10^{-18}$ m^2/s)	*m*-Xylene ($\times 10^{-19}$ m^2/s)
HZSM-5	0.5	4.7	6.3	3.8
HZSM-5M	0.5	5.3	0.7	1.1
HZSM-5 [17]	1	60	6.5	7

m-xylene (0.68 nm) [24]. Note that the ratio of diffusion coefficients between *p*-, *o*-, and *m*-xylene was reported as 1000:10:1 by Mirth et al. [17] and as 1000:1:1 used in a mathematical model to describe the enhanced para-selectivity by Wei [25]. Because a zeolite with smaller crystals (0.5 μm) was used in this study, the diffusion coefficient of *p*-xylene measured is, as expected, lower than that on large crystals reported in the literature [20,26,27], which has been ascribed to "surface barrier effects" [28,29], that is, the existence of a physisorbed precursor state outside of the zeolite particle [30]. After silylation of the zeolite, the diffusivity of *p*-xylene remained unchanged, whereas the diffusion coefficients of *o*-xylene and *m*-xylene decreased by approximately 10- and 4-fold, respectively, demonstrating that silylation leads to narrowing/blocking of a fraction of the pore openings of the zeolite and to a more marked diffusional restriction for molecules with large kinetic diameter. It is noteworthy to mention that modification of the zeolite increases the difference in diffusivity among *p*-xylene and *o*-xylene or *m*-xylene, as was also found with very large crystals of HZSM-5 [14].

3.2. *o*-Xylene isomerization

Typical time-resolved IR spectra of *o*-xylene isomerization over the parent zeolite at 473 K are shown in Fig. 3. With increasing time on stream, the intensity of IR bands at 3745 and 3606 cm^{-1} decreased, indicating increasing coverage with reactants and products. In parallel, the intensity of IR bands characteristic of *o*-xylene at 1497, 1468, and around 3000 cm^{-1}, as well as the band of the perturbed bridging hydroxyl groups at approximately 3168 cm^{-1}, increased. In addition, the band at 1610 cm^{-1}, characteristic of *m*-xylene, increased with the slower rate. All bands reached a steady-state value after approximately 7 min time on stream. The composition of xylenes in the gas phase and the concentrations of sorbed xylenes in the parent zeolite during *o*-xylene isomerization as a function of time on stream are compiled in Figs. 4 and 5, respectively. The rapid initial increase of *o*-xylene on the surface is related to the increased concentration in the reactor after admission of the reactant. The slower increase in the *m*-xylene concentration is related to the fact that its accumulation in the pores is the primary product of isomerization. At steady state, its rate of formation equals the rates of its isomerization to *p*-xylene and its diffusion out of the pores. The *o*- and *m*-xylene were adsorbed primarily in the zeolite pores at 473 and 523 K. The minor surface concentration of *p*-xylene resulted from the sorption equilibrium of *p*-xylene formed during reaction over the zeolite. Because *m*-xylene has approximately twice the partial pressure of *p*-xylene under the conditions of the experiment (0.8 mbar), the significantly higher concentration (about 5- to 10-fold greater)

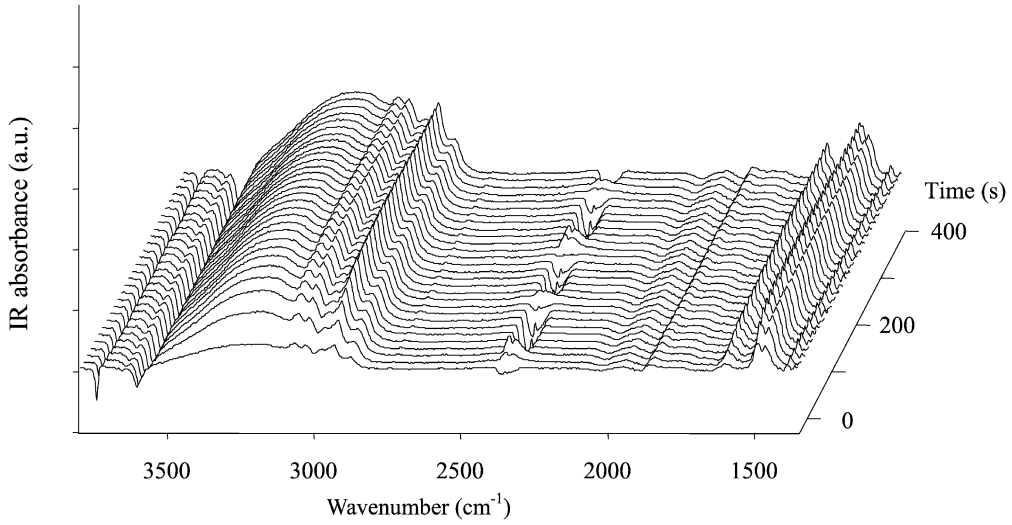

Fig. 3. Time resolved IR spectra of *o*-xylene isomerization with HZSM-5 at 473 K.

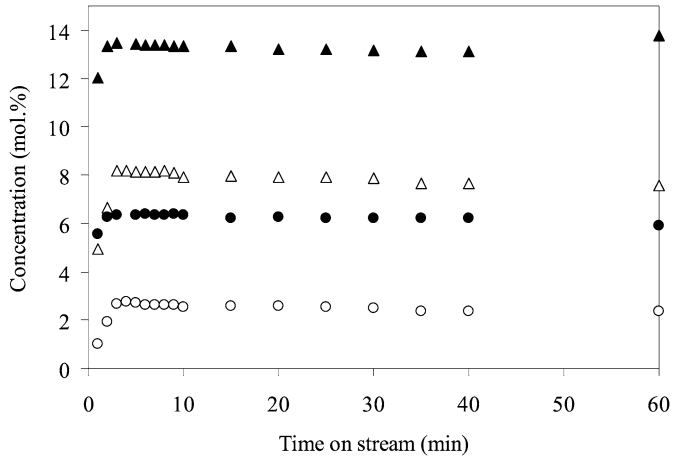

Fig. 4. Product composition during *o*-xylene isomerization over HZSM-5 at 473 and 523 K as a function of time on stream. ((●, ○) *p*-xylene and (△, ▲) *m*-xylene. Open symbols at 473 K and filled symbols at 523 K.)

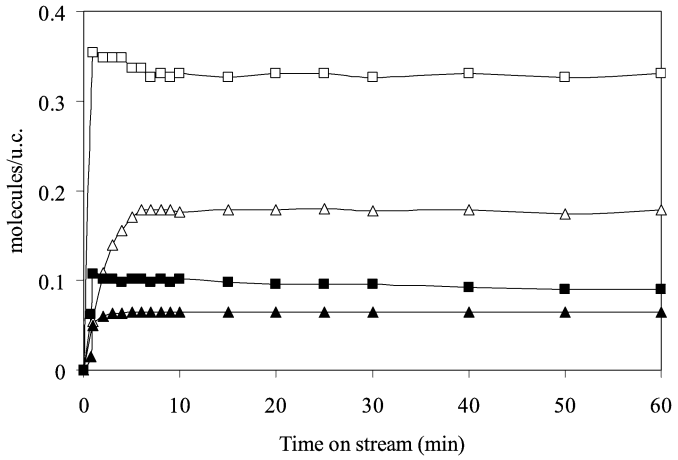

Fig. 5. Concentration of sorbed xylenes during *o*-xylene isomerization over HZSM-5 at different temperatures as a function of time on stream. ((■, □) *o*-xylene and (△, ▲) *m*-xylene. Open symbols at 473 K and filled symbols at 523 K.)

inside the pores indicates the retention of *m*-xylene through diffusional constraints. Increasing the isomerization temperature to 523 K led to a shorter transient. For *o*-xylene isomerization over HZSM-5, increasing the reaction temperature from 473 to 523 K led to an increased ratio of *p*-xylene to *m*-xylene from 0.32 to 0.48 in the reaction gas phase and an increased reaction rate from 3.6×10^{-3} to 7.0×10^{-3} molecule/site's under the steady-state conditions. Note also that the concentration of adsorbed xylenes decreased, but the ratio between sorbed *m*-xylene and *o*-xylene increased from 0.55 to 0.77 as the temperature was raised from 473 to 523 K.

Figs. 6 and 7 compare the product composition and surface concentration of sorbed molecules during *o*-xylene isomerization over the silylated zeolite (HZSM-5M) as a function of time on stream. A markedly longer transient period (compared with that of the parent zeolite) and lower reaction rates of 1.8×10^{-3} molecule/site's at 473 K and 2.8×10^{-3} molecule/site's at 523 K were observed. In the gas phase, higher ratios of

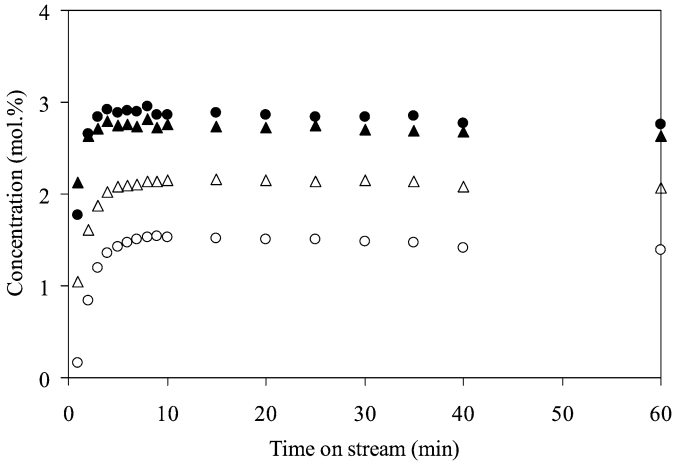

Fig. 6. Product composition during *o*-xylene isomerization over HZSM-5M at different temperatures as a function of time on stream. ((●, ○) *p*-xylene and (△, ▲) *m*-xylene. Open symbols at 473 K and filled symbols at 523 K.)

p-xylene to *m*-xylene (i.e., 0.71 at 473 K and 1.1 at 523 K), were observed. As with the parent zeolite, only *o*- and *m*-xylene were observed in the pores of the silylated zeolites. The ratio of adsorbed *m*-xylene to *o*-xylene was 1.0 at 473 and 523 K, higher than that of the parent zeolite. Note that the xylene loadings were generally lower in the silylated zeolite than in the parent zeolite.

3.3. *p*-Xylene isomerization

The composition of the surface species in the pores of the zeolites and the products in the gas phase during *p*-xylene isomerization are compiled in Table 2. A short transient period was observed for *p*-xylene isomerization over the parent zeolite, indicating that equilibration in the pores was slower than the pressure step-up in the reactor. With an increase in reaction temperature from 473 to 523 K, the reaction rates increased from 3.8×10^{-3} to 7.9×10^{-3} molecule/site's, and the ratio of *o*-xylene to *m*-xylene in the reactor increased from 0.16 to 0.28. Only *p*- and *m*-xylene were adsorbed in HZSM-5 and HZSM-5M. Increasing the isomerization temperature from 473 to 523 K led to an increase in the ratio of sorbed *m*- to *p*-xylene on HZSM-5 from 0.75 to 1.13.

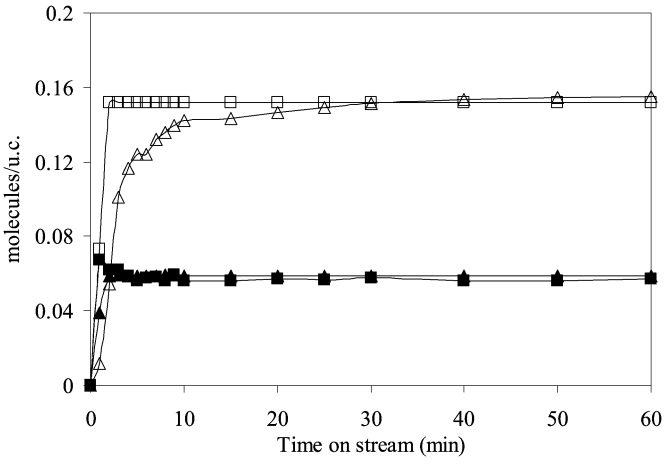

Fig. 7. Concentration of sorbed xylenes during *o*-xylene isomerization over HZSM-5M at different temperatures as a function of time on stream. ((■, □) *o*-xylene and (△, ▲) *m*-xylene. Open symbols at 473 K and filled symbols at 523 K.)

As the reaction temperature increased, the rate of *p*-xylene isomerization increased from 1.9×10^{-3} molecule/site's at 473 K to 4.2×10^{-3} molecule/site's at 523 K with HZSM-5M. The ratio of *o*- to *m*-xylene in the gas phase was 0.33 at 473 K and 0.39 at 523 K. In addition, a higher ratio of adsorbed *m*- to *p*-xylene (1.13 at 473 K and 1.6 at 523 K) was observed.

3.4. *m*-Xylene isomerization

The xylene composition during *m*-xylene isomerization in the gas phase and in the zeolite pores is listed in Table 3. For *m*-xylene isomerization, markedly longer transient periods and lower reaction rates (e.g., 2.2×10^{-3} molecule/site's at 473 K and 4.8×10^{-3} molecule/site's at 523 K) were observed, attributed to the lower diffusivity of *m*-xylene compared with *p*- or *o*-xylene. Silylation led to decreased reaction rates of *m*-xylene isomerization to 1.2×10^{-3} molecule/site's at 473 K and 2.2×10^{-3} molecule/site's at 523 K. Note that the ratio of *p*-xylene to *o*-xylene in the gas stream over the parent zeolite remained constant during the transient period and increased slightly from 2.3 at 473 K to 2.4 at 523 K.

m-Xylene was the predominate adsorbed species on HZSM-5 and HZSM-5M. The minor concentrations of *o*- and *p*-xylene adsorbed resulted from the adsorption of the product molecules present in the gas phase over the zeolite in the CSTR-type reactor. Note that (approximately) the same concentration of *p*-xylene was formed in *m*- and *o*-xylene (see Table 4) isomerization in the gas phase, and thus the same surface concentrations of *p*-xylene were observed in both reactions.

Table 2
Concentration of xylenes adsorbed on the zeolites and in the gas phase during *p*-xylene isomerization

Sample	Temperature (K)	Reaction rate (mol $[H^+]^{-1}$ S^{-1})	Sorbed xylenes (mol/u.c.)			Xylenes in gas phase (mol%)		
			o-	*m*-	*p*-	*o*-	*m*-	*p*-
HZSM-5	473	3.8×10^{-3}	0	0.29	0.40	1.3	8.1	90.6
	523	7.9×10^{-3}	0	0.14	0.15	4.3	15.2	80.5
HZSM-5M	473	1.9×10^{-3}	0	0.32	0.23	0.7	2.1	97.2
	523	4.2×10^{-3}	0	0.16	0.10	1.7	4.4	93.9

Table 3
Concentration of xylenes adsorbed on the zeolites and in the gas phase during *m*-xylene isomerization

Sample	Temperature (K)	Reaction rate (mol $[H^+]^{-1}$ S^{-1})	Sorbed xylenes (mol/u.c.)			Xylenes in gas phase (mol%)		
			o-	*m*-	*p*-	*o*-	*m*-	*p*-
HZSM-5	473	2.2×10^{-3}	0.01	0.45	0.02	1.5	95.3	3.2
	523	4.8×10^{-3}	0.01	0.15	0.02	3.4	89.4	7.2
HZSM-5M	473	1.2×10^{-3}	0.01	0.40	0.02	0.7	97.7	1.6
	523	2.2×10^{-3}	0.01	0.10	0.01	1.3	95.7	3.0

Table 4
Concentration of xylenes adsorbed on the zeolites and in the gas phase during *o*-xylene isomerization

Sample	Temperature (K)	Reaction rate (mol $[H^+]^{-1}$ S^{-1})	Sorbed xylenes (mol/u.c.)			Xylenes in gas phase (mol%)		
			o-	*m*-	*p*-	*o*-	*m*-	*p*-
HZSM-5	473	3.6×10^{-3}	0.33	0.18	0.03	90.0	7.6	2.4
	523	7.0×10^{-3}	0.09	0.07	0.02	80.5	13.2	6.3
HZSM-5M	473	1.8×10^{-3}	0.15	0.15	0.02	96.4	2.1	1.5
	523	2.8×10^{-3}	0.06	0.06	0.01	94.4	2.7	2.9

4. Discussion

4.1. On the mechanism of xylene isomerization

With zeolite catalysts, xylene isomerization can occur via an intermolecular or an intramolecular mechanism. The preference for a specific mechanisms depends on the pore structure, the concentration of the reactants, and the density and type of the acid sites. A high density of acid sites, the presence of Lewis acid sites, a high reactant concentration, and large pore volume favor the bimolecular mechanism [31–33]. In contrast, the opposing boundary conditions favor a monomolecular mechanism.

In agreement with the literature [33–35], all observations suggest that isomerization of the xylenes on HZSM-5 proceeds via the intra-molecular reaction mechanism. Thus, two consequences can be derived: (a) The intrinsic isomerization rate must be directly proportional to the concentration of the isomer adsorbed, and (b) the intramolecular reaction mechanism requires that primary (*m*-xylene) and secondary isomerization products exist in the pores during the isomerization of *p*- and *o*-xylene. In contrast, if an intermolecular mechanism prevails, then all isomers can be (kinetically) primary isomerization products independent of the reacting isomer.

Both consequences of the intramolecular isomerization route have been observed experimentally. The rate of isomerization has been found to be directly proportional to the concentration of adsorbed *m*-xylene [17]. The situation is more complex for *p*-xylene and *o*-xylene isomerization, because some of the products may be retained in the pores. Initially, the surface concentration of the reactant determines the sum of the rates of observable gas-phase product formation and the accumulation of sorbed xylene isomers. (Bulky molecules such as *m*-xylene are formed via isomerization but cannot desorb.) At steady state, the rate of gas-phase product formation is determined by sum of the concentrations of the sorbed reactant and products.

With respect to the second point, we would like to emphasize that the in situ IR spectra demonstrate for isomerization of *o*- and *p*-xylene that *m*-xylene is visible as the only product and that it accumulates markedly in the zeolite pores early while on stream. Note that the low surface concentrations of *p*-xylene observed during *o*-xylene isomerization resulted from adsorption of the molecules formed in the reaction. Thus, the slightly increasing selectivity to the product with the higher diffusivity is caused by the accumulation of *m*-xylene in the pores and its increased isomerization rate. The direct conversion occurs only between *p*-xylene and *o*-xylene to *m*-xylene; that is, xylene isomerizes via a 1,2-methyl shift. At short times on stream, the relative rates of diffusion determine the product composition; as time on stream progresses, the increased concentration of retained *m*-xylene leads to some additional contribution to the *p*-xylene formation rate as the sorbed *m*-xylene is isomerized.

Although the present experiments do not prove it, we suggest in analogy to *o*- and *p*-xylene that also *m*-xylene isomerizes via the unimolecular reaction mechanism. Because the selectivity to *p*-xylene was $69 \pm 1\%$ for the parent and silylated zeolites, we conclude that the higher *p*-selectivity is caused by a more favorable transition state of the *m*-xylene/*p*-xylene reaction compared with the *m*-xylene/*o*-xylene reaction (see also [17]). It is interesting to note that the marginal changes in selectivity with reaction temperature strongly suggest that this is an entropy-controlled process; that is, not the differences in the energetic barriers to differentiate between reaction pathways, but rather the differences in probability to achieve a particular transition state.

4.2. Impact of pore mouth blocking and pore mouth modification

Silylation of HZSM-5 with TEOS leads to the passivation of Brønsted and Lewis acid sites on the external surface and preferentially in the pore mouth region of HZSM-5 zeolites [13]. In addition, the changes in the diffusivity (studied by the frequency response method) of toluene indicate a drastic narrowing or practical blocking of larger patches of pore openings [36], which induces a longer and more tortuous pathway for molecules entering and leaving the zeolite particle. As a consequence, smaller zeolite particles show the characteristics of much larger ones, which has been shown to lead to enhanced *p*-selectivity [37].

For all three isomerization reactions studied, the silylated zeolite had lower catalytic activity than the parent material. This finding may be related to two different mechanisms. The acid sites at the pore mouth of the zeolite are eliminated by silylation, and, consequently, the overall concentration of acid sites is reduced. Because the reaction order of the isomerization under these conditions is close to 1, the direct proportionality of the reaction rate to the acid site concentration leads in turn to lower activity. However, the blocking of pores also increases the tortuosity of the channel system, which is expected to lead to more pronounced diffusional constraints for reactants and products.

The subtle differences observed for the three isomers allow us to unequivocally identify the role of the two effects

of silylation on xylene isomerization at low conversion levels. For *m*-xylene isomerization, lower catalytic activity and lower *m*-xylene loadings were observed for HZSM-5M compared with the parent zeolite. Compared with findings on HZSM-5, the coverage of *m*-xylene on HZSM-5M decreased by only 11%, and the acid site concentration after silylation decreased by 23% [13]. It is interesting to note that the concentration of Al^{3+} is significantly higher in the lattice close to the pore openings, which form Brønsted acid sites, than in the inner part of the crystal. (Assuming a cubic particle with a size of 0.5 μm, each pore consists of about 250 unit cells. If the Al^{3+} is randomly substituted, then only 1.6% of the Al atoms should be located in the first unit cell after the pore entrance.) Based on the difference in site coverage and the decreased site concentration, we conclude that the acid sites at the pore mouth must make less of a contribution to the overall adsorption of xylenes. This finding is in perfect agreement with a recent study on the details of the sorption of benzene in HZSM-5 [38] showing that the sites at the pore mouth are saturated at a higher equilibrium pressure compared to sites inside the pores; that is, in general they have a lower heat of adsorption for aromatic molecules. This effect is rationalized by the weaker contribution of the van der Waals forces in a less constrained environment. However, it also has been shown that the steric constraints are relaxed at the pore mouth, and, therefore, the energetic contribution of the direct interaction of benzene with the Brønsted acid sites compared with the nonlocalized interaction with the pore walls is much stronger than that with Brønsted acid sites inside the pores [38]. In general, two energetic contributions—the directed interaction between Brønsted acidic SiOHAl groups and the electron pair donor function of the molecules (basic function) and the nondirected van der Waals interactions between the zeolite pore walls and the sorbate—can be differentiated. For benzene, the nonlocalized interaction with the pore walls controls the sorption energetically, whereas the localized interaction with the bridging hydroxy groups contributes to only a minor degree [38]. Because the impact of the steric constraints will be even more pronounced for the xylenes isomers compared with benzene, the direct interaction of xylene with the Brønsted acid sites at the pore mouth would be expected to be stronger than that with the Brønsted acid sites inside the ZSM-5 pores.

This is drastically reflected in the differences between the catalytic activity of the parent and silylated zeolites. Although the coverage of *m*-xylene decreased by only 11%, the rate of *m*-xylene isomerization decreased by 45%. The observation strongly suggests that the Brønsted acid sites at the pore entrance are markedly more active than the sites in the zeolite channels. At present, we have no indication that this difference is related to variations in acid strength, and thus we suggest that it is caused by the ability of the xylene molecules to reach an unconstrained equilibrium position with the protons of the strong Brønsted acid sites at the pore entrance, as has been observed for benzene. Such an unconstrained complex should allow a more facile proton transfer than that occurring inside the ZSM-5 pores.

The selectivity to *p*-xylene was constant at $69 \pm 1\%$ for all catalysts and all temperatures, suggesting that the molecules converted at the more active pore mouth sites face a similar (sterical) restriction in the transition state. This finding also confirms that the sites in the inner part of the pores were not modified by silylation.

For *o*- and *p*-xylene isomerization, the situation was similar at first glance; i.e., silylation decreased the rate of isomerization by approximately 50%. It is important to note, however, that the decreased concentration of adsorbed reactants (i.e., 57% for *p*-xylene and 48% for *o*-xylene) was markedly higher than for *m*-xylene. In addition, in situ IR spectroscopy showed a marked accumulation of *m*-xylene in the zeolite pores, suggesting that during the initial (transient) reaction, *m*-xylene is formed at a rate higher than the subsequent isomerization or diffusion out of the pores. Although we cannot suggest a quantitative model at the moment, we would like to emphasize that the diffusion and reaction pathways differ markedly for HZSM-5 and HZSM-5M. For the unmodified sample, not only is the reactivity of the sorbed species higher, but also more of the *m*-xylene adsorbed is able to desorb. After modification, all Brønsted acid sites at the pore entrance are eliminated, minimizing the likelihood chance that the *m*-xylene formed can desorb without a relatively long diffusion pathway. Note that at 523 K, the equilibrium value for *m*-xylene adsorption at 20 mbar was approximately 0.2 mol/u.c., whereas approximately the same concentration was reached during *p*-xylene isomerization when only 0.8 mbar *m*-xylene was present in the reactor. This clearly shows that *p*- and *o*-xylene isomerization is a product diffusion-controlled process.

In the context of the related shape-selective toluene disproportionation on HZSM-5, Zheng et al. [14,36] found that silylation effectively suppressed the secondary isomerization of xylene on Brønsted acid sites in the pore mouth. Based on our results presented here, we conclude that instead it is the unconstrained diffusion of *m*-xylene formed near the pore entrances of the unmodified zeolites that is suppressed by silylation.

5. Conclusion

The results of our parallel kinetic measurements and the time-resolved in situ IR spectroscopy demonstrate that xylenes isomerize via an intramolecular pathway catalyzed by Brønsted acid sites. For all catalysts studied, the catalytic activity is related to the concentration of reactants on the acid sites. Diffusion limitations markedly influence that coverage. The catalytic activity of the Brønsted acid sites at the pore entrance is significantly higher than the catalytic activity of such sites inside the pores of the ZSM-5 zeolite. These Brønsted acid sites are postulated to be part of the crystalline structure with an overall geometry of HZSM-5. However, the somewhat more open environment at the pore entrance leads to an unconstrained adsorption structure of the aromatic molecules and hence to more facile protonation. It is interesting to note that the differentiation in the catalytic activities of these sites was the strongest by far with the sterically most demanding molecule (i.e., *m*-xylene).

Measurement of the concentrations of reactants and products in modified and unmodified materials showed that the isomerization of *m*-xylene is controlled by transition state selectivity; that is, the faster-diffusing reaction products are found in only minor concentrations inside the pores. Note that this finding is in agreement with the low partial pressure of both reactants in the CSTR reaction cell. In contrast, the selectivity in *o*- and *p*-xylene isomerization is controlled by the retention and accumulation of *m*-xylene in the pores; i.e., the reaction is a product diffusion–influenced process.

Silylation effectively blocks larger patches of pore openings for the aromatic molecules, enhancing the differences in the diffusivity of *p*-, *o*-, and *m*-xylene, whereas the inner pores are hardly influenced. In line with the different reaction mechanisms for reaching a particular product composition, silylation has markedly different affects on *m*-xylene and *o*- and *p*-xylene isomerization.

For *m*-xylene isomerization, the more active sites at the pore mouth are blocked, leading to lower activity. However, the inner pores, and hence the geometrically probable transition states, are hardly influenced, leading to near-identical distributions for *p*- and *o*-xylene. In contrast, for *p*- and *o*-xylene, the higher tortuosity of the zeolite crystals reduces the evolution of *m*-xylene and leads to a higher relative concentration of *m*-xylene in the pores at higher reaction temperatures and with more effective silylation. It is this difference in the retention, rather than the difference in chemistry at the pore mouth sites, that is responsible for the enhanced shape selectivity.

Acknowledgments

Partial financial support from the Bayerische Forschungsverbund Katalyse (FORKAT II) is gratefully acknowledged. S. Zheng thanks the Deutsche Forschung Gemeinschaft and the Ministry of Education of the People's Republic of China for providing a visiting scholarship.

References

[1] J. Weitkamp, Solid State Ionics 131 (2000) 175.
[2] W.W. Kaeding, G.C. Barile, M.M. Wu, Catal. Rev.-Sci. Eng. 26 (1984) 597.
[3] J. Cejka, B. Wichterlova, Catal. Rev. 44 (2002) 375.
[4] T. Tsai, S. Liu, I. Wang, Appl. Catal. A 181 (1999) 355.
[5] S.M. Csicsery, Zeolites 4 (1984) 202.
[6] D.H. Olson, W.O. Haag, ACS Symp. Ser. 248 (1984) 275.
[7] J.-H. Kim, T. Kunieda, M. Niwa, J. Catal. 173 (1998) 433.
[8] M. Niwa, N. Katada, T. Murakami, J. Phys. Chem. 94 (1990) 6441.
[9] M. Niwa, N. Kanada, Y. Murakami, J. Catal. 134 (1992) 340.
[10] M. Niwa, S. Kato, T. Hattori, Y. Murakami, J. Chem. Soc., Faraday Trans. 1 80 (1984) 3135.
[11] Y.H. Yue, Y. Tang, Y. Liu, Z. Gao, Ind. Eng. Chem. Res. 35 (1996) 430.
[12] C. Gründling, G. Eder-Mirth, J.A. Lercher, J. Catal. 160 (1996) 299.
[13] S. Zheng, H.R. Heydenrych, A. Jentys, J.A. Lercher, J. Phys. Chem. B 106 (2002) 9552.
[14] S. Zheng, H.R. Heydenrych, H.P. Roeger, A. Jentys, J.A. Lercher, Top. Catal. 22 (2003) 101.
[15] R.W. Weber, K.P. Möller, M. Unger, C.T. O'Conner, Microporous Mesoporous Mater. 23 (1998) 179.
[16] R.W. Weber, K.P. Möller, C.T. O'Conner, Microporous Mesoporous Mater. 35 (2000) 533.
[17] G. Mirth, J. Cejka, J.A. Lercher, J. Catal. 139 (1993) 24.
[18] G. Mirth, J.A. Lercher, J. Catal. 132 (1991) 244.
[19] G. Mirth, J.A. Lercher, J. Catal. 147 (1994) 199.
[20] J. Kärger, D.M. Ruthven, Diffusion in Zeolite and Other Micro-Porous Solids, Wiley, New York, 1992.
[21] C.L. Cavalcante, D. Ruthven, Ind. Eng. Chem. Res. 34 (1995) 185.
[22] J. Xiao, J. Wei, Chem. Eng. Sci. 47 (1992) 1123.
[23] J. Xiao, J. Wei, Chem. Eng. Sci. 47 (1992) 1143.
[24] A. Corma, V. Fornes, L. Forni, F. Marquez, J. Martinez-Triguero, D. Moscotti, J. Catal. 179 (1998) 451.
[25] J. Wei, J. Catal. 76 (1982) 433.
[26] G. Müller, T. Narbeshuber, G. Mirth, J.A. Lercher, J. Phys. Chem. 98 (1994) 7436.
[27] L. Song, L.V.C. Rees, Microporous Mesoporous Mater. 35–36 (2000) 301.
[28] J. Kärger, S. Vasenkov, Microporous Mesoporous Mater. 85 (2005) 195.
[29] J. Kärger, M. Bülow, G.R. Millward, J.M. Thomas, Zeolites 6 (1986) 146.
[30] A. Jentys, H. Tanaka, J.A. Lercher, J. Phys. Chem. B 109 (2005) 2254.
[31] S.M. Csicsery, D.A. Hickson, J. Catal. 19 (1970) 386.
[32] K.M. Wang, J.H. Lunsford, J. Catal. 24 (1972) 262.
[33] M. Guisnet, N.S. Gnep, S. Morin, Microporous Mesoporous Mater. 35–36 (2000) 47.
[34] A. Cortes, A. Corma, J. Catal. 51 (1978) 338.
[35] A. Corma, E. Sastre, J. Chem. Soc., Chem. Commun. (1991) 173.
[36] S. Zheng, A. Jentys, J.A. Lercher, J. Catal. 219 (2003) 310.
[37] S. Zheng, H. Tanaka, A. Jentys, J.A. Lercher, J. Phys. Chem. B 108 (2004) 1337.
[38] A. Jentys, R.R. Mukti, H. Tanaka, J.A. Lercher, Microporous Mesoporous Mater. (2005), in press.